


RESEARCH ARTICLE

Eddy generation in a large, deep dimictic freshwater lake in ice-free period

Alexei V. Kouraev ^{1*}, Elena A. Zakharova,^{2,3} Andrey G. Kostianoy,^{4,5} Nicholas M.J. Hall,¹ Anna I. Ginzburg,⁴ Frédérique Rémy,¹ Roman E. Zdrovenov,⁶ Andrey Ya Suknev⁷

¹Université de Toulouse, LEGOS (CNES/CNRS/IRD/UT3), Toulouse, France; ²EOLA, Toulouse, France; ³Institute of Water Problems, Russian Academy of Sciences, Moscow, Russia; ⁴Shirshov Institute of Oceanology, Russian Academy of Sciences, Moscow, Russia; ⁵S.Yu. Witte Moscow University, Moscow, Russia; ⁶Northern Water Problem Institute, Karelian Center of the Russian Academy of Sciences, Petrozavodsk, Russia; ⁷Great Baikal Trail (GBT) Buryatiya, Ulan-Ude, Russia

Abstract

We address eddy generation in the middle part of Lake Baikal—a large freshwater dimictic lake in Siberia, where river discharge, wind influence and coastline shape impact horizontal water exchange. We use satellite remote sensing, historical observations and in situ data to follow the different stages of warm and cold anticyclonic eddy generation before and after vertical overturn; an aspect that has received little attention in previous works. Thermal satellite images for 1998–2022 indicate a stable repeating seasonal pattern which is classified into stage of eddy generation and development. Field observations complement satellite imagery to characterize the vertical structure of the eddies. The main source of eddy generation is the outflow from Barguzin Bay which interacts with the coastline. Subsequent eddy generation is driven by density gradients and geostrophic adjustment. In summer, this outflow is dominated by river inflow and lead to the formation of warm anticyclonic eddies. After autumnal vertical overturn, the outflow is forced by the wind bringing cold water from the bay to Middle Baikal and creating cold anticyclonic eddies. We suggest that in the autumn, when the surrounding water cools to a temperature below about 4°C, these cold eddies sink and transform into intrathermocline lens-like eddies that persist under ice and can later create giant ice rings on the Baikal ice cover.

Eddies are a ubiquitous feature of open oceans, inland seas, and lakes. They are effective agents of horizontal and vertical water mixing with diameters that vary from a few hundred meters to over 200 km and lifetimes from days to years. Understanding the driving factors and patterns of eddy generation and development is essential for a wide variety of limnological and oceanographical studies.

Eddies are formed through a variety of mechanisms: baroclinic and barotropic instability, interaction of the flow with the bottom, shoreline or strait, geostrophic adjustment of a convectively mixed layer, surface fluxes of heat and momentum,

and local forcing such as river flow or melting ice. Eddies can manifest as intrathermocline lenses (e.g., Meddies, *see* Kostianoy and Belkin 1989), meandering large-scale frontal currents (e.g., Gulf Stream rings, *see* Robinson 1983), island and headland wakes, dipoles, and multipoles (Fedorov and Ginzburg 1986; Ivanov and Ginzburg 2002), and sub-mesoscale eddies (Kostianoy et al. 2018; Zatsepin et al. 2019).

The key mechanism addressed in this study is eddy generation behind capes due to alongshore current separation. Such eddies have often been observed on satellite images over oceans and seas where there is an irregular coastline (*see* e.g., Pattiaratchi, James, and Collins 1986; Alpers et al. 2013; Aleskerova et al. 2021). Although this mechanism is similar in seas and in lakes, some of the factors driving the generation and further development of eddies can differ, and in here we address some specific circumstances for lake Baikal.

There are two factors that distinguish eddies in freshwater dimictic lakes such as Baikal from oceanic eddies. First, water density in these lakes is mostly defined by water temperature,

*Correspondence: alexei.kouraev@univ-tlse3.fr

Associate editor: Sally MacIntyre

Data Availability Statement: Data are available on request from the authors. Satellite imagery has been processed by the European Space Agency (ESA) SNAP software, which is publicly available (<https://step.esa.int/main/download/snap-download/>, ESA 2024).

while the salinity contribution is negligible. Second, since fresh water has maximum density at about 4°C, dimictic lakes that have two vertical overturning events per year present two contrasting density configurations. In summer, between the vernal and autumnal overturns, warmer water is lighter than colder water and temperature decreases with depth for stable stratification. After autumnal overturn water colder than 4°C is lighter and resides in the upper layer, reversing the temperature stratification. This means that for the same region there will be warm-core eddies in summer, and cold-core eddies in winter. They will have different temperature/density 3D structure, and drivers for their generation for the same area may vary seasonally. While warm-core eddies in various lakes of the world are relatively well studied, cold-core lake eddies and the seasonal transition from one type of eddy to another have received much less attention.

In this paper, we consider horizontal water exchange and eddy generation in Lake Baikal in Siberia. We focus on a specific region in Middle Baikal: Barguzin Bay and the open abyssal part in Middle Baikal itself (Fig. 1). This large region has a complex coastline, and is significantly affected by river inflow, wind, and horizontal water temperature gradients. It presents a good case for multifactor eddy generation that could be applied to many similar lakes.

The mean current along the Baikal coast is cyclonic (anti-clockwise), and in addition each part of the lake also has its own system of cyclonic gyres (Afanasyev and Verbolov 1977; Shimaraev and Verbolov 1998). Our study region is located between two such large-scale circulation cells, where intermittent outflow from the bay leads to mesoscale and sub-mesoscale variability in surface currents that has not been addressed in detail in previous publications.

Studies that use thermal infra-red satellite imagery show that the warm circular structures have been observed to occur frequently in the open part of Middle Baikal (Le Core 1998; Troitskaya et al. 2015; Sutyryna 2016). Most authors suggest that the formation of these eddies is associated with the outflow of warm water from Barguzin Bay, modified by the coastline (the Svyatoy Nos Peninsula). However, the factors affecting the intensity of the outflow, its seasonal variability, the transition from warm to cold eddies, and the 3D structure of these eddies have received little attention.

The study region is known for the frequent occurrence of warm lens-like (double-convex form) intrathermocline eddies beneath the ice cover that may manifest themselves on lake ice as giant ice rings with a diameter of 5–7 km (Granin et al. 2015; Kouraev et al. 2016, 2019) These eddies are similar to the well-known Mediterranean “Meddies” in the North Atlantic Ocean that are related to rapid intrusion of large volume of water with different density and propagate at a depth of about 1 km. Other similar eddies (very often called lenses) have been observed in almost all parts of the World Ocean (Kostianoy and Belkin 1989). The fact that giant ice rings have been also found in Lake Hovsgol in Mongolia and Lake

Teletskoye in Altai, Russia (Kouraev et al. 2016, 2019) suggests that intrathermocline eddies exist in many other dimictic seasonally frozen deep lakes.

The timing and driving forces of intrathermocline eddy formation requires further clarification. For Middle Baikal our analysis of thermal satellite imagery in autumn 2015 showed that an eddy was formed in ice-free conditions in late autumn due to wind-driven outflow of cold water from the bay along the peninsula. This eddy later led to the formation of a giant ice ring in 2016. We suggested that wind-driven water outflow after autumnal overturn and before ice formation is the main driver for eddies under ice in this region as well as potentially in many other places where eddies and ice rings were observed (Kouraev et al. 2019). In this paper, we use satellite imagery archives to further explore eddy generation in late autumn and early winter before ice formation.

We assess factors affecting eddy generation and development in Middle Baikal over an extended period in the ice-free season. Barguzin Bay is enclosed by a peninsula and we hypothesize that pulsating outflow of water with different density from the bay to the open part is the main mechanism of eddy generation. Specifically, we assess the relative importance of river inflow and wind in Barguzin Bay, how these factors influence on the outflow from the bay, how their impact varies in time and space, and how additional factors such as coastline shape and topography contribute to their variability. We focus on seasonal and interannual variability of surface currents and generation and development of eddies, frequency, timing, horizontal and vertical structure, and location of the eddies. To do this, we make use of new datasets acquired from satellite remote sensing and complement them with historical meteorological observations and data from our field surveys and moorings.

Site description and methods

Site description

Lake Baikal, a dimictic and seasonally ice-covered lake, is the deepest (maximum depth 1642 m, average depth 744 m) and one of the largest (length about 650 km and width up to 80 km) lakes in the world. The study region (Fig. 1) exemplifies a situation where multiple factors affect the horizontal current field leading to eddy generation. Barguzin Bay is bounded to the north by the Svyatoy Nos Peninsula, which disrupts and channels water exchange between the bay and open part of the lake and also significantly modifies the wind field. Shallow depths less than 50 m extend for just 2 km from the coast near Cape Krestoviy, but in the bay proper they occupy almost half the bay surface (up to 12 km distance from the eastern coast). At the exit from the bay lies the extensive abyssal plain of Middle Baikal with depths of more than 1500 m.

The Barguzin River flows into the bay at a mean rate of 3.9 km³ yr⁻¹ (Garmaev and Khristophorov 2010) with high interannual variability (see Supporting Information Fig. S1). Most of the water comes during spring flood (33% of annual

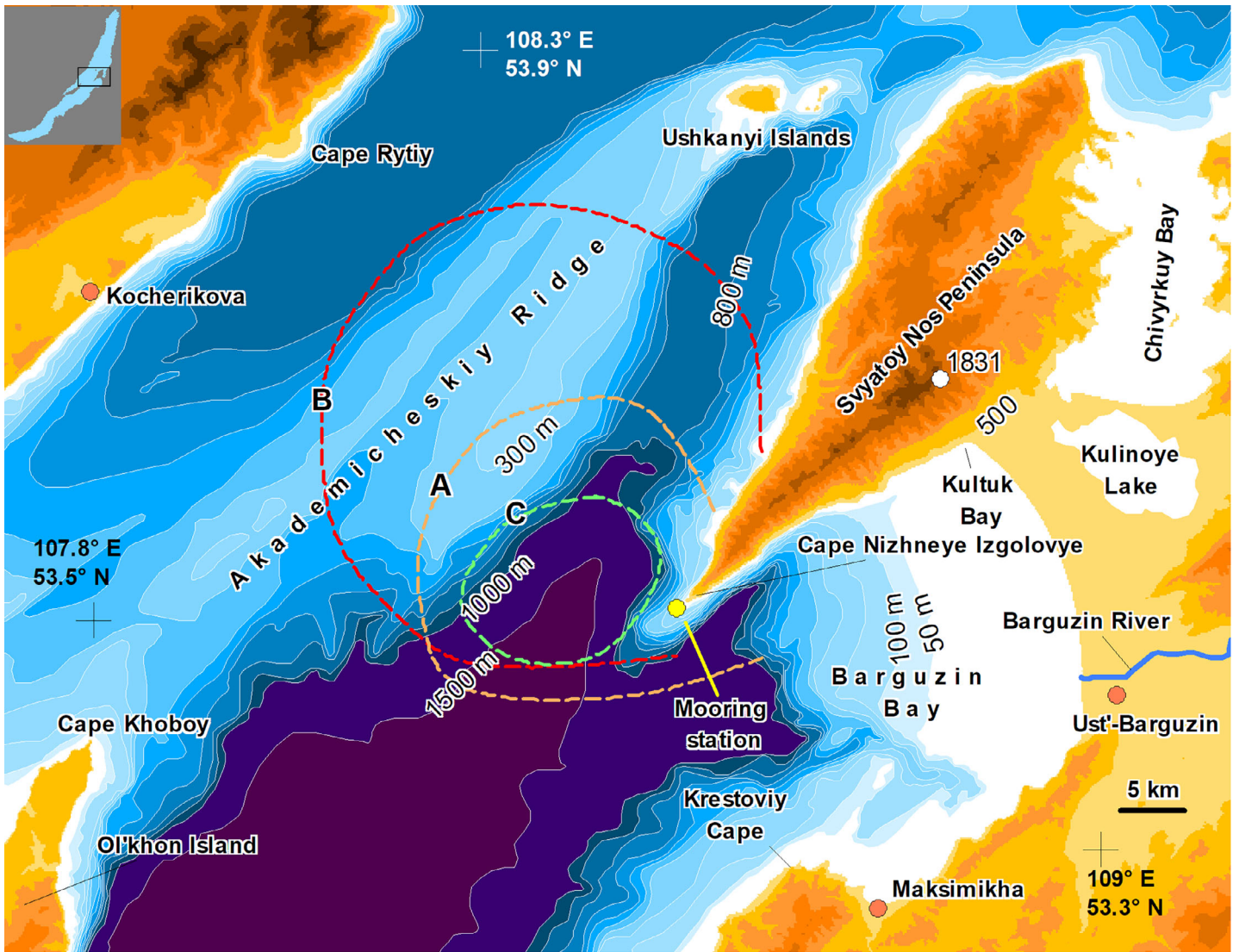


Fig. 1. Region of study. Isobaths (relative to the Lake Baikal level) are shown every 100 m between 100 and 1000 m and relief is shaded every 200 m between 500 and 1700 m absolute sea level. Dashed lines show typical location of eddy boundaries (see Section “Structure and spatial location of eddies”): A, early stages; B, maximal eddy development; C, region of main occurrence of giant ice rings.

inflow) and summer and autumnal rains (57%). Large shallow areas in the bay and water inflow from the Barguzin River create conditions for significant temperature contrasts between the bay and open lake. In summer and autumn, river water and shallows are warmer than water in deep regions and in late autumn they are colder. This difference in temperature leads to large density gradients, especially when water from the bay is injected to the open part of Middle Baikal.

Another important driver of water exchange is the wind. Lake Baikal is long and deep, surrounded by mountain ridges. The large thermal inertia of the lake and the continental climate lead to differences in air temperature and pressure between the lake and surrounding land and strong seasonal and diurnal wind variability during both warm and cold

seasons. Existing literature (Grechishev and Mamontov 1964; Rzhaplinskiy and Sorkina 1977; Rusinek et al. 2012) indicates that in the Middle Baikal region one can identify four main wind regimes. Two winds are oriented along the lake axis—*Verkhovik* from the northern tip of the lake and *Kultuk* from the southwestern tip, and two winds—*Gornaya* and *Barguzin*—across the lake (in this paper we will use wind names in italics, to avoid confusion with similar geographical names). *Verkhovik* and *Kultuk* may affect lake surface state over large distances. The cross-lake wind *Gornaya* comes from the northwest where downslope air movement in narrow mountain valleys results in strong winds with speed up to 40 m s^{-1} . The other cross-lake wind is the easterly *Barguzin* coming from Barguzin Bay.

Lake Baikal experiences two vertical overturning events per year, resulting in homogeneous vertical distribution of water temperature down to 250 m depth (Rusinek et al. 2012). This change in vertical stratification is important for the current field because it changes the thickness of the upper mixed layer and its response to wind forcing. Our data (see Supporting Information Table S1) indicate that near the Nizhneye Izgolovye Cape spring overturn is observed in the first half of June and autumnal overturn in the second half of November.

Every winter Lake Baikal is ice-covered for several months. Ice can grow to 100–110 cm thickness and presents a stable surface without ice drift, isolating water from the direct influence of the wind. For the study region in 2017–2020, ice formation was observed between late December and early January, and ice break-up between late April and early May (see Supporting Information Table S1).

Wind field variability and spatial patterns

We have analyzed wind regimes and air temperature using data from five meteorological stations of the Russian Hydrometeorological Service: Ust'-Barguzin, Uzury, Bol'shoy Ushkaniy Island, Solnechnaya, and Khuzhir (2005–2022). Meteorological stations provide useful information on the wind regime, but they are affected by local orographic conditions and are less representative for the open part of the lake. To reveal spatial wind patterns over large areas of Middle Baikal we used radar satellite imagery. Synthetic Aperture Radar is an active side-looking microwave radar technique that is not affected by clouds, does not require the presence of sunlight, and is highly sensitive to water surface roughness (Stopa et al. 2017; Villas Bôas et al. 2019; Kostianoy and Lavrova 2022). Calm water reflects radar signal away from the satellite receiving antenna, resulting in low return echo and is typically shown as black or dark gray on radar images. When the wind blows over water surface, increased surface roughness alters reflective and emissive properties of water, and regions with elevated roughness provide a higher return echo, shown as light gray or white. We have analyzed Level 1 Ground Range Detected High-Resolution Interferometric Wide swath mode Sentinel-1A and -1B images in vertical-vertical and vertical-horizontal polarizations for 2014–2022 (over 800 images). These images have a spatial resolution of 5×20 m. The images were processed using European Space Agency (ESA) SNAP software (ESA SNAP 2024).

Spatial and temporal evolution of eddies

Satellite imagery in the thermal range is one of the best ways to assess water dynamics by analyzing the spatial distribution of water surface temperature. Data include thermal infrared and visible bands from Landsat 5 (Thematic Mapper sensor, bands 3 and 6), Landsat 7 (Enhanced Thematic Sensor + sensor, bands 3 and 62) and Landsat 8 (Operational Land Imager and Thermal Infrared Sensor sensors, bands 4 and 10). Over 300 images for 1998–2022 were analyzed. Using a visual pattern recognition approach (Jain and Duin 2004; Gibson 2011)

and analyzing shape, position, size, and temperature distribution inside and outside the eddies, we have detected patterns of horizontal water exchange and classed them into phases. The main analysis was done using thermal bands, but visible, near- and short-wave infrared bands and radar imagery were also used. Thermal bands were processed following approach described in the Landsat Product Website (2024).

Satellite thermal infrared data give an estimate of water temperature distribution, but only at the surface. Remote sensing can reveal numerous features such as front, eddies, and filaments at scales of 1–10 km, but in situ measurements at this scale are rare (Villa Bôas 2019). To better understand the 3D structure of eddies, we organized boat cruises in summer (July 31, 2017) and early autumn (September 10, 2019) in the region offshore from Cape Nizhneye Izgolovye. Stations were placed at intervals of about 3 km to resolve the eddies in the region where eddies are usually found in summer. We used RBR (Canada) TD Duet temperature/depth logger (2 Hz sampling, temperature accuracy $\pm 0.002^\circ\text{C}$, resolution $< 0.0005^\circ\text{C}$, pressure accuracy 0.85 m, and resolution 1.7 cm). Observations were made from a boat, with the logger suspended from a manual winch. The sampling depth was from the surface down to 200 m in July 2017 and 400 m in September 2019. The maximum depth varied for each station due to boat drift under the influence of wind and waves.

Currents near the cape

In July 2017, a subsurface mooring station near the cape was installed in a region of 100 m depth, 1.2 km southwest of the cape (see Fig. 1) to investigate water exchange between the bay and the open part of Middle Baikal. The rope was anchored on the bottom and had a flotation buoy at the top, 5–7 m below the surface. On this rope, we installed several RBR (Canada) Solo T temperature loggers (accuracy 0.002°C , resolution $< 0.0005^\circ\text{C}$) and a SeaHorse Tilt Current Meter made by Vitalii Sheremet, Okeanolog, Model SH1p70M based on Lowell Inc MAT-1 Logger (Sheremet 2010; Maio et al. 2016) with three-axis accelerometer (0.002 g accuracy) and compass. The current meter operated at 30 m depth and provided current speed and direction every 5 min between July 31, 2017 and September 4, 2018. Previous winter campaigns have shown that SeaHorse data provide measurements of speed and direction comparable with those from an electromagnetic current meter (Kouraev et al. 2019).

Results

Wind field variability and spatial patterns

Data from five meteorological stations located in the Middle Baikal region confirm the known strong seasonal variability of the wind regime in the ice-free period (Rusinek et al. 2012). Between May and August winds from all directions are mostly weak but in October–December the average wind speed doubles ($3\text{--}6$ m s^{-1} vs. $1\text{--}3$ m s^{-1}). *Gornaya* (wind from northwest) is observed at stations on the western coast and in the open part

of the lake. In June–August, its frequency of occurrence is comparable to that of winds from other directions, though the typical wind speed is much higher up to $7\text{--}12\text{ m s}^{-1}$. In October–December, *Gornaya* intensifies to a steady $16\text{--}24\text{ m s}^{-1}$ with gusts up to 29 m s^{-1} and becomes the prevailing wind on the western coast. At the eastern coast in Barguzin Bay, there are two main winds: *Barguzin* from southeast at $2\text{--}5\text{ m s}^{-1}$ dominating in cold period and at $1\text{--}3\text{ m s}^{-1}$ west to southwesterly wind from the open part of the bay dominating in warm period. While *Gornaya* is a strong wind that does not last long, *Barguzin* is relatively weak but persistent. In the cold period it is usually uninterrupted for 11–17 d, and it can blow for 1 month (2009, 2012) or more (2014) with only some short interruptions.

Radar imagery complements data from meteorological stations providing for the analysis of spatial heterogeneity of the wind field over open parts of Middle Baikal. Figure 2 illustrates the influence of the main winds and shows their spatial distribution. The wind speed and direction from meteorological stations (also shown on Fig. 2) are consistent with the radar images.

Barguzin appears to generate a fan-shaped outflow that is about 8 km wide near the coast and reaches 20 km width offshore (Fig. 2a). A typical feature for mountain-surrounded lakes is that every valley descending to a lake works as an “injection point” for the wind. The length and area of each valley, the width, shape and topography of valley mouth, and the wind speed and duration determine the wind footprint on the water surface. In Fig. 2a, there are several small-scale sources of wind in the southeastern part of Barguzin Bay. Together with *Barguzin*, they influence the water surface over the exit region from the bay and this influence further expands over 90 km from the source. Several more northwesterly winds from west coast valleys were also detected. *Barguzin* can coexist with the along-lake northeastern wind (Fig. 2b). In such cases, these two winds affect most of Middle Baikal.

Gornaya (Fig. 2c,d) originates from small valleys along the western coast of Maloye More, but the main air outflow is concentrated in the coastal lowlands. Several wide bands of wind join together and create a 40-km-wide band that ultimately reaches the opposite coast. Depending on atmospheric circulation, this wind may either enter Barguzin Bay and reach its eastern coast (Fig. 2c) or be oriented more to the southeast and in this case will not affect Barguzin Bay (Fig. 2d).

When there are two (Fig. 2e) or three (Fig. 2f) types of winds simultaneously affecting almost all the Middle Baikal, the limits of influences of each wind can be clearly detected from convergence lines. Radar images also show that the wind impact on the lake surface is spatially heterogeneous at scales of just several kilometers and observations at coastal stations are often unable to capture this.

Spatial and temporal evolution of eddies

Analysis of satellite thermal imagery has shown that every year there is a typical repeating pattern of seasonal evolution

of water exchange between Barguzin Bay and the open part of Middle Baikal, which initiates eddy generation behind the Nizhneye Izgolovye cape. We have classed this pattern into 12 phases (Fig. 3; Table 1) characterized by specific temporal and spatial development. We have broadly grouped them onto four main stages referring to the “age” of the eddies—Nascent, Developing, Mature, and Decaying/New cold eddy—with specific phases within each stage.

Nascent stage

Phase 1 (not shown on Fig. 3) starts after ice break-up. Several drifting floes of ice remain. The surface water temperature in the bay and outside is $1\text{--}2^\circ\text{C}$. During *Phase 2*, in a narrow 1–2 km band along the coast the water starts to warm up ($8\text{--}12^\circ\text{C}$). It is transported anticlockwise by the general circulation along the coast to the northern part of the bay and at the same time spreads out in the bay. Water in the wide part of the bay and outside is mostly homogeneous, with temperatures close to 4°C .

During *Phase 3*, there is an increase of warm ($12\text{--}17^\circ\text{C}$) water extent in the bay. The main transport is along the coast to the northern part of the bay and beyond, but depending on wind conditions there could be other warm plumes spreading in different directions into the bay. A sharp boundary between warm water and cold and homogeneous water can be detected from thermal satellite images. During *Phase 4*, warm water ($9\text{--}20^\circ\text{C}$) reaches the cape and forms a narrow tongue flowing to the southwest and west onto the open part of Middle Baikal. In *Phase 5*, the outflow tongue increases in width (3.7 km and a temperature of $14\text{--}17^\circ\text{C}$ for Fig. 3d) and closes the clockwise loop outside the cape. This is the first fully formed anticyclonic warm eddy. It is about 15 km in diameter.

Developing stage

During *Phase 6*, the initial warm eddy near the cape increases in horizontal extent. Successive arrivals of warm water from the bay near the cape (width of outflow is 4.4–5 km for Fig. 3e) create a second clockwise-oriented filament inside the eddy, with the appearance of two nested spirals (Fig. 3e). Other filaments also extend from the central part of the bay (Fig. 3f), possibly as a result of drift of warm river water. During *Phase 7*, depending on wind conditions, solar heating, and the arrival of warm river water, further warming leads either to nested spirals (*Phase 7A*, similar to *Phase 6A*), or, more typically, to a well-developed large (diameter 40 km) homogeneous warm eddy (*Phase 7B*).

The evolution of this mesoscale anticyclonic eddy is accompanied by the formation on its periphery of elements of shear instability. They are filaments (shingles) which are directed in the opposite direction to the rotation of the eddy or the associated sub-mesoscale cyclones. These cyclones with diameters of about 5–7 km can be seen on the southern, northeastern, and eastern peripheries of the anticyclone.

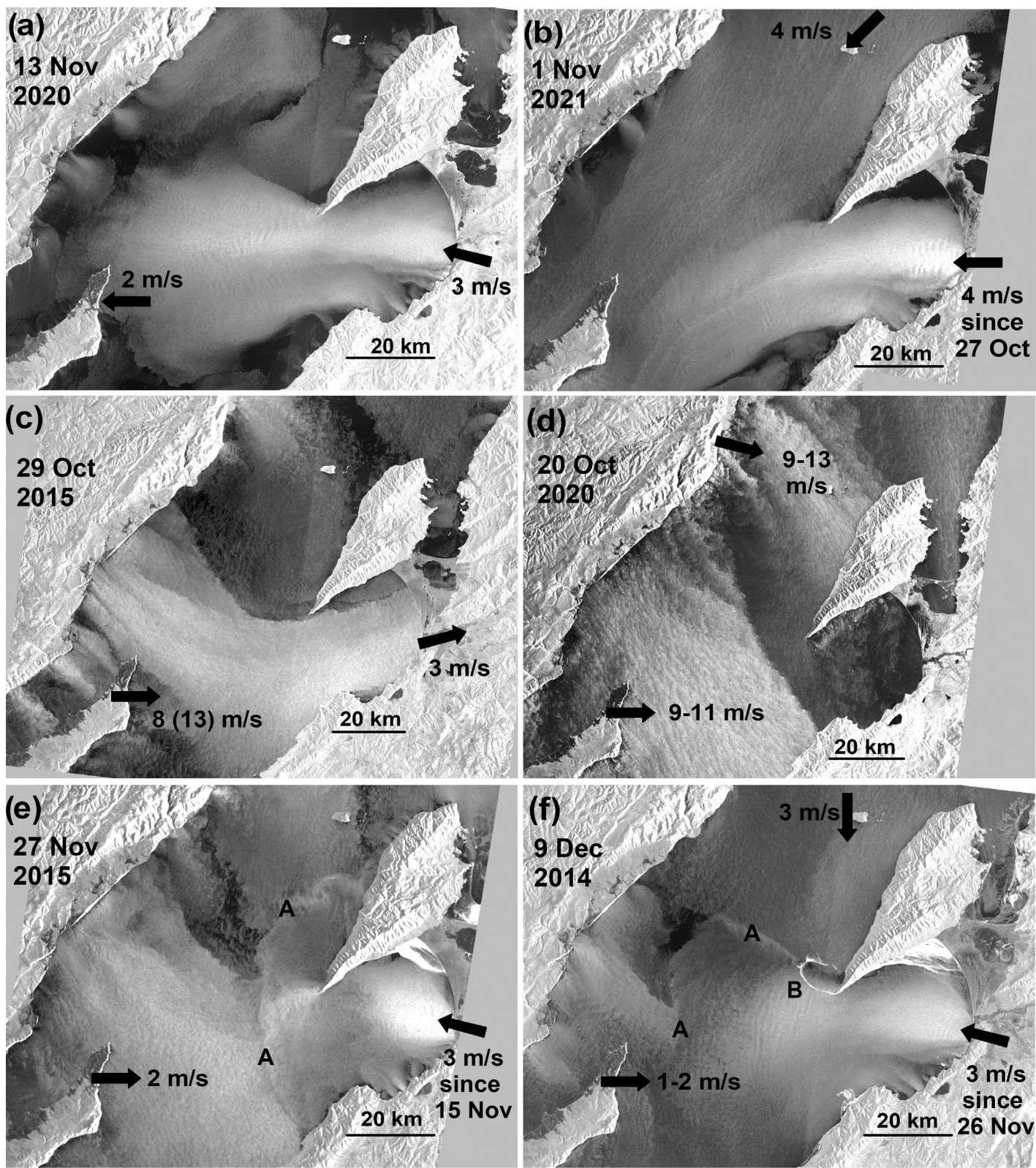


(Figure legend continues on next page.)

Mature stage

In September, during *Phase 8*, the eddy outside gets larger. Warm water in the bay either continues to flow along the coast (*Phase 8A*), or extends over the whole bay area creating a second eddy in the bay. This second eddy may have a colder center (*Phase 8B*) or a uniform temperature (*Phase 8C*). In the latter case, both eddies have similar size (30–35 km) and temperature. During *Phase 9*, the outside eddy continues to grow and its temperature starts to decrease. Its form may change due to wind and currents, and in some cases the eddy may reach the opposite western coast.

Decaying/new cold eddy stage

Between mid-October and early November, the eddy cools and its form evolves (*Phase 10*). Water outside the eddy is often 4°C or less. Plumes of water colder than 4°C coming from the river and from the coastal regions start to form. During *Phase 11*, the warm eddy outside the cape may still exist with temperatures close to 4°C. The eddy is often hidden on the thermal imagery by the lateral advection of water colder than 4°C (which is now lighter than the surrounding warmer water and thus overlies the warm eddy). In the image of November 25, 2015 (Fig. 3n), we observe a fan-shaped pool of colder water (label A, 0–0.5°C) over warmer water with a temperature of 1–2°C (label B), concealing the warm eddy remnants below.

Inside the bay, negative air temperature and strong winds lead to rapid water cooling. Ice may start to form along the coast and in the northern part of the bay. A stream of very cold water along the coast goes first to the northern part of the bay, then to the cape and finally forms a cold clockwise-oriented tongue entering Middle Baikal near the cape. This situation is similar to Phases 4 and 5, except that the intrusion brings now colder, but again lighter, water.

Phase 12 is characterized by extremely cold air and very strong winds that can affect the water until the ice cover is fully formed. Continuing outflow of cold water creates a closed clockwise eddy near the cape. This new cold eddy has initial size similar to the spring eddy. It can be detected from thermal imagery (see Kouraev et al. 2019 for the Landsat image from December 4, 2015) and from visible and radar imagery. The image in the visible range (Fig. 3o) shows thin young ice drifting out from the bay and creating two nested lines near the cape. One is smaller and fully closed in the center and the second is larger, not fully closed and partly hidden by clouds.

In late autumn, clouds over the lake often limit the detection and analysis of eddy development in the visible and thermal ranges. Radar imagery, which is not sensitive to clouds, illustrates the birth of a new cold eddy (Fig. 3p) on December 26, 2016. Most of the bay was covered by thin and smooth nilas ice, typically seen as black on radar images (Smirnov 2011). The floating forms of young ice, such as ice needles or grease ice, compacted onto shuga ice are seen as very white on radar images (Bushuev, Volkov, and Loshilov 1974; Smirnov 2011). They serve as passive tracers that depict surface currents. Shuga was transported from the bay outwards, turning clockwise after the cape and creating a spiral of ice. As in the warm anticyclone case, elements of shear instability form at the cold anticyclone periphery. Shingles can be seen to the north and west, and an associated cyclonic eddy in the bay to the south (Fig. 3p).

In summary, a warm eddy is created every year in July near the cape. It grows during August and September and cools in September–October. By November it is no longer visible. Then a cold eddy is created in November–December. This cold eddy is similar in form and genesis to the warm eddy in spring.

3D structure of eddies from satellite imagery and boat surveys

Two cross-eddy in situ profile surveys corresponding to different phases of eddy evolution, together with simultaneous thermal and visible satellite images are employed to investigate the 3D eddy structure. The first survey was carried out on July 31, 2017, and is complemented by Landsat 8 images in thermal and visible ranges 3 d later (Fig. 4). A large clockwise (anticyclonic) eddy was created following warm water outflow from Barguzin Bay. The thermal satellite image shows that the eddy had a temperature of 17–18°C and its core was colder at 16°C. On the visible image the outer limit of the eddy is seen as a 6–7 km wide band with increased reflectance. This high reflectance could be associated with phytoplankton or other suspended matter that is concentrated along the flow lines, frontal zones, and regions of surface convergence (Fedorov and Ginsburg 1992; Lavrova et al. 2011; D'Asaro et al. 2018). Reflectance could thus possibly serve as a tracer for eddy currents. The eddy diameter is about 24 km and its shape corresponds to *Phase 6* in which outflow from the cape extends to the open part, turns clockwise and forms a closed eddy.

Vertical profiles along the transects A–C and D–E are similar and show a well stratified water column. The thermocline is located at 5–7 m depth, with an upper mixed layer at 13–

(Figure legend continued from previous page.)

Fig. 2. Examples of wind influence on Sentinel-1A and -1B radar images. (a) Barguzin; (b) joint influence of Barguzin and Verhovik; (c) strong Gornaya entering Barguzin Bay; (d) strong Gornaya blowing south–southeast; (e) simultaneous influence of Barguzin and Gornaya, creating line with heterogeneous roughness (marked A) where winds converge; (f) combination of Barguzin, Gornaya, and Verhovik, A indicates line of elevated roughness where winds converge, B indicates line of young ice (shuga) transported from Barguzin Bay and depicting an anticyclonic (clockwise) eddy. Dates for Sentinel-1B images are given in local time (Greenwich Mean Time + 8, about 7 h in the morning local time). Where available and relevant, direction (arrows) and wind speed at the meteorological stations Ust'-Barguzin, Uzury and Bol'shoy Ushkaniy are given for the closest corresponding local time. North is always oriented upward.

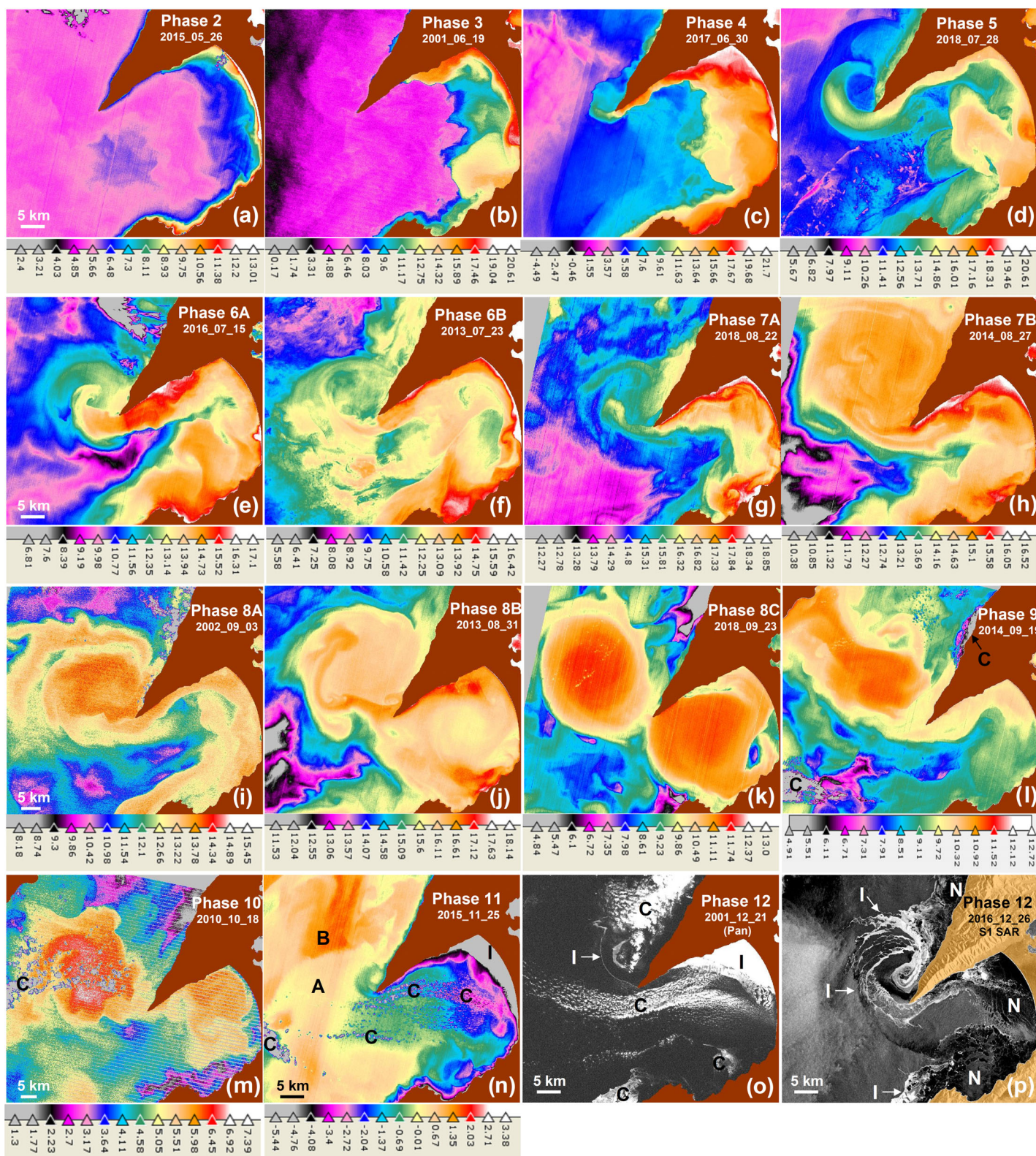


Fig. 3. Examples of typical water surface temperature from Landsat thermal (a–n), and pan-chromatic (o) and Sentinel-1A WV radar images (p) for different phases of Nascent (a–d), Developing (e–h), Mature (i–l), and Decaying (m–p) stages. Spatial scale is the same for images except (o). North is up. C, clouds; I, ice; N, nilas ice (smooth surface, seen as dark on radar image).

Table 1. Timing and main characteristics of phases of eddy generation. See Supporting Information Table S2 for statistics on temporal boundaries and years and number of satellite images for each specific phase.

Phase	Time	Brief description
Nascent stage		
1	Early May to mid-May	Initial state after ice melt
2	Second half of May to beginning of Jun	Warming in 1–2 km wide band. Warm water reaches northern part of the bay
3	Second decade of Jun	Warm water area grows, extends beyond the northern part of the bay and in the bay itself
4	Mid-Jun to end of Jun	Warm tongue reaches the cape and extends to Middle Baikal
5	Early Jul to second decade of Jul	First fully closed loop of warm eddy beyond the cape
Developing stage		
6	Mid-Jul to end of Jul	Eddy is spreading out. Consecutive pulses create nested filaments
7	Beginning of Aug to end of Aug	Growing. Nested spirals or large eddy with homogeneous temperature
Mature stage		
8	Early Sep to late Sep	Formation of eddy in the bay, eddy outside grows
9	Mid-Sep to early Oct	Eddy outside is getting colder, its size continues to increase
Decaying/new cold eddy stage		
10	Mid-Oct to early Nov	Water in coastal zone and the river inflow are colder than 4°C. Eddy outside continues to cool down
11	End of Oct to end of Nov	New tongue of cold water goes to the cape and out to Middle Baikal; warm eddy still exists
12	Mid-Nov to end of Dec	New cold eddy is formed outside of the cape (similar to <i>Phase 5</i>)

15°C, several degrees colder than surface temperature observed by satellite. On the most western and southern stations the deep layer at 100–150 m is cold (3.6–4°C).

We suggest that the eddy is constantly supplied by outflow from Barguzin Bay, with an associated downward inclination of isotherms and an increase of vertical separation of isotherms. The thickness and volume of each layer thus increases, especially over the range 9–13°C.

Another survey on September 10, 2019 was limited to the outer boundary of the eddy. Vertical profiles show that the thermocline in this late autumn period is deeper, at about 30–40 m as a result of gradual cooling and vertical convection following a decrease in air temperature and an increase in wind forcing (*see* Supporting Information for results and description). Data across the associated sub-mesoscale cyclonic eddy at the southern edge of the anticyclonic eddy show that this associated eddy affects water down to 80 m depth. The characteristics and parameters of eddies in summer and autumn are presented in Table 2.

Currents near the Nizhneye Izgolovye Cape

Exchange between Barguzin Bay and open part of Middle Baikal which plays an important role in eddy formation can be evaluated using observations of current speed and direction from a current meter installed near the cape where the main outflow comes from the bay is situated. The direction of the

current spanned 90° between 157.5° and 247.5°. As the main outflow from Barguzin Bay is oriented along the coast of the Svyatoy Nos Peninsula, it maintains this direction for several kilometers before turning northwest and then north toward the open part of Middle Baikal. The mooring station is located slightly north of this main current, and therefore records the direction of entrainment of water from neighboring regions to this main current.

When ice cover is present, the current speed is at its slowest with the median value of 7.5 cm s⁻¹ and peak values never exceeding 15 cm s⁻¹. Even in the middle of winter under stable ice cover and with no direct wind influence on the water surface, there is still a current with a slow but constant speed at least 4–6 cm s⁻¹. This shows that the general anticlockwise coastal water transport (Afanasyev and Verbolov 1977; Shimaraev and Verbolov 1998), typical for all three parts of Lake Baikal, does not stop even in the midwinter. After ice break up, as the winds are weak during May–August, currents only increase slightly (8–9 cm s⁻¹). In September–November, the stronger winds lead to increased current speeds increase with a median speed of 24.5 cm s⁻¹ in November and 41 cm s⁻¹ in December and early January.

Discussion

Our results based on satellite, historical and in situ data have made it possible for the first time to assess eddy

Table 2. Main characteristics of eddies in different seasons.

	Summer eddy	Autumn eddy	Winter eddy*
Timing and duration	May–Jun (young) July–Oct (max) About 6 months	Oct–mid-Nov (young) Nov–Dec (max) About 2 months	Jan–May About 5 months
Temperature/density as compared to surrounding water	Warmer/lighter	Colder/lighter	Warmer/denser in the upper part and colder/lighter in the lower part
Form	Intrusion, pushing colder water downward (inclination of isotherms) and increasing volume of water with specific temperature (larger vertical distance between isotherms)	n.i. probably the same as in summer	Double-convex lens-like form
Top of eddy surface manifestation	Yes	Yes	No. Intrathermocline (submerged or touching ice)
Driver	Successive outflow from the bay, intrusion of water with different density and geostrophic adjustment	Same as for summer eddy	Evolution of autumn eddy
Main outflow driver	River discharge	Wind stress	Sustained by inertia
Current speed (at the cape)	8–9 cm s ⁻¹	24–41 cm s ⁻¹	7–8 cm s ⁻¹
Diameter	35–40 km	15–20 km	6–7 km on top, 12 km at neutral depth
Rotation direction	Anticyclonic (clockwise)	Anticyclonic (clockwise)	Anticyclonic (clockwise)
Current velocity inside the eddy	n.i.	n.i.	3 d for full rotation, almost no current in the center, fast current at eddy periphery
Thermocline depth	5–7 m on 31 Jul 2017, 30–40 m on 10 Sep 2019	n.i.	45–50 m (many years)
Depth of water layer affected by eddy	More than 160 m (in 2017)	n.i.	More than 200 m (in 2016 and 2017)
Development with time	Grows in time, displaces	Same as summer eddy	Probably adapts in shape in the beginning of winter but mostly stays the same
Stationarity	May travel, but mostly related to the cape and may be trapped by bathymetry	Same as summer eddy	May travel, but often is trapped by bathymetry in the heads of underwater depressions
Observation from satellite data	Thermal (main), also passive tracers in visible and near infrared. Obstacles: cloud cover (except radar)	Thermal (main), also passive tracers (young ice) in visible, near infrared and radar. Obstacles: cloud cover (except radar)	Giant ice rings as surface manifestation of stationary intrathermocline eddies (visible, near infrared, thermal, and radar). Obstacles: cloud cover (except radar), unstable/drifted ice cover in spring

Abbreviation: n.i., no information.

*Based on data from (Kouraev et al. 2016, 2019).

generation and development between June and December in several years and to describe horizontal and vertical structure of eddies in a freshwater dimictic lake both before and after

autumnal overturn. Interactions between the bay, isolated by the peninsula, and the deeper open part of Middle Baikal lead to dynamic water exchange and complex current structure.

Drivers of water exchange and eddy generation

Among the main factors defining the intensity of the outflow from the bay to Middle Baikal are river inflow and wind stress over the lake surface. Analysis of wind fields shows that surface currents in the bay and water exchange with Middle Baikal are governed not only by *Barguzin* (blowing from the bay) but also, somewhat counterintuitively, by *Gornaya*. *Barguzin* leads to outflow of water near the cape, generation of anticlockwise (cyclonic) water circulation in the bay and formation of clockwise (anticyclonic) eddies behind the cape (see also Fig. 2f, line B). Although it originates on the opposite coast, *Gornaya* also strongly influences the surface currents. With distance between the western and eastern coasts of 75–100 km, *Gornaya* with the speed of 5–10 m s⁻¹ will reach the opposite coast in 2–5 h. When *Gornaya* fully or partly enters the southern part of the bay, it creates currents oriented east or northeast, pushing and piling up water in the bay and ultimately (a) enhancing anticlockwise (cyclonic) circulation in the bay and (b) increasing outflow to Middle Baikal near the cape. So, both *Barguzin* and *Gornaya* are implicated in increased outflow from the bay to Middle Baikal.

The respective contribution of wind stress and river inflow is highly variable and these two factors are well separated in time (Fig. 5). Maximum river discharge is observed between June and August, when more than half of the total annual discharge comes to bay. The wind, on the other hand, is calm during the summer months. The influence of the wind rapidly increases in November–December, at the same time as the river flow is decreasing.

For *warm eddies* in summer, sequences of thermal images show that they are generated by successive outflows of warmer water from Barguzin Bay to Middle Baikal around the cape, confirming the conclusions of earlier works (Le Core 1998; Sutyryna 2016). Comparison of river discharge and wind speed with current speed at the mooring station (Fig. 5) shows that the main driver for increased outflow and generation of warm eddies in summer is river discharge. Additional input of warmer water may come from shallow regions. A large part of the bay is relatively shallow and water there warms faster in summer. When this warmer water is transported to Middle Baikal by the general cyclonic (anticlockwise) basin-scale circulation, it also contributes to the injection of water with different density and thus to eddy generation.

For *cold eddies* formed in November–December (Fig. 5) the main driver is strong wind bringing cold water from Barguzin Bay to the warmer open part of Middle Baikal. The peak values of current speed in November–December are closely related to intense winds in November and especially in December. When wind is steady, large volumes of water leave the bay and enter Middle Baikal. In November–December 2015, *Barguzin* was blowing almost uninterruptedly for 2 months. This event led to strong outflow of water from the bay, the formation of an eddy and an unusually early giant ice ring in 2016 (Kouraev et al. 2019).

As observed in oceans and seas, the formation of an eddy behind a cape is related to the detachment of a coastal current that follows an irregular coastline. In both summer and autumn, the outflow from the bay and temperature gradient between the incoming and surrounding water lead to the generation of anticyclonic eddies near the cape. The initial generation factor is the blocking of the coastal current by the peninsula and formation of eddies behind the cape. However if this were the only reason, these eddies would be short-lived. The intrusion from the bay of a large volume of water with different temperature, and thus density lower than the water in open part of the lake, is essential for the longevity of the eddy. Both warm and cold eddies are anticyclonic, because they are *light-core* eddies. If not for Coriolis effect, this lighter water would spread out evenly, creating layers of increased thickness. The Coriolis force deviates the spreading current to the right until the current is geostrophically adjusted and is perpendicular to the radial pressure gradient associated with the thermal/density anomaly.

Further evolution of cold eddies in winter

Cold eddies formed in late autumn do not dissipate, but subduct beneath the lake surface when surrounding water cools down, and persist below the ice. In our previous study we suggested that outflow from the bay in late autumn was the main driver for subsurface intrathermocline eddies that later lead to the formation of giant ice rings (Kouraev et al. 2016, 2019, 2021). That initial hypothesis was based on thermal satellite imagery only for one autumn 2015. It is now corroborated by at least 15 out of 25 yr (1998–2022) with confirmed cases of cold eddy formation observed in November–December (see Supporting Information Table S2). The outflow from the bay, as a precursor to eddy formation is thus confirmed as a perennial feature that repeats over many years. It appears to be the fundamental mechanism for horizontal water exchange and eddy generation.

The cold eddy formed after autumnal overturn evolves until stable ice cover forms in January. Further cooling of neighboring water under ice will lead to a situation where the eddy becomes warmer than the surrounding water and thus denser. The cold eddy below the ice will remain undisturbed by wind, and due to geostrophic adjustment, it will adopt a double-convex lens form, centered vertically at the neutral density depth. The main characteristics of intrathermocline eddies are summarized in Table 2.

If such an intrathermocline eddy remains stationary it will eventually lead to an accelerated ice melt at the eddy boundary and the formation of giant ice rings at the ice surface in spring. Thin and unstable ice in the ice ring region is difficult to detect from the surface. Together with the unpredictability of ice ring locations from year to year this represents a significant danger for people traveling on Lake Baikal (Leech 2018; Kouraev et al. 2019, 2021). This stipulates the need for further studies of this phenomenon and communication of results for

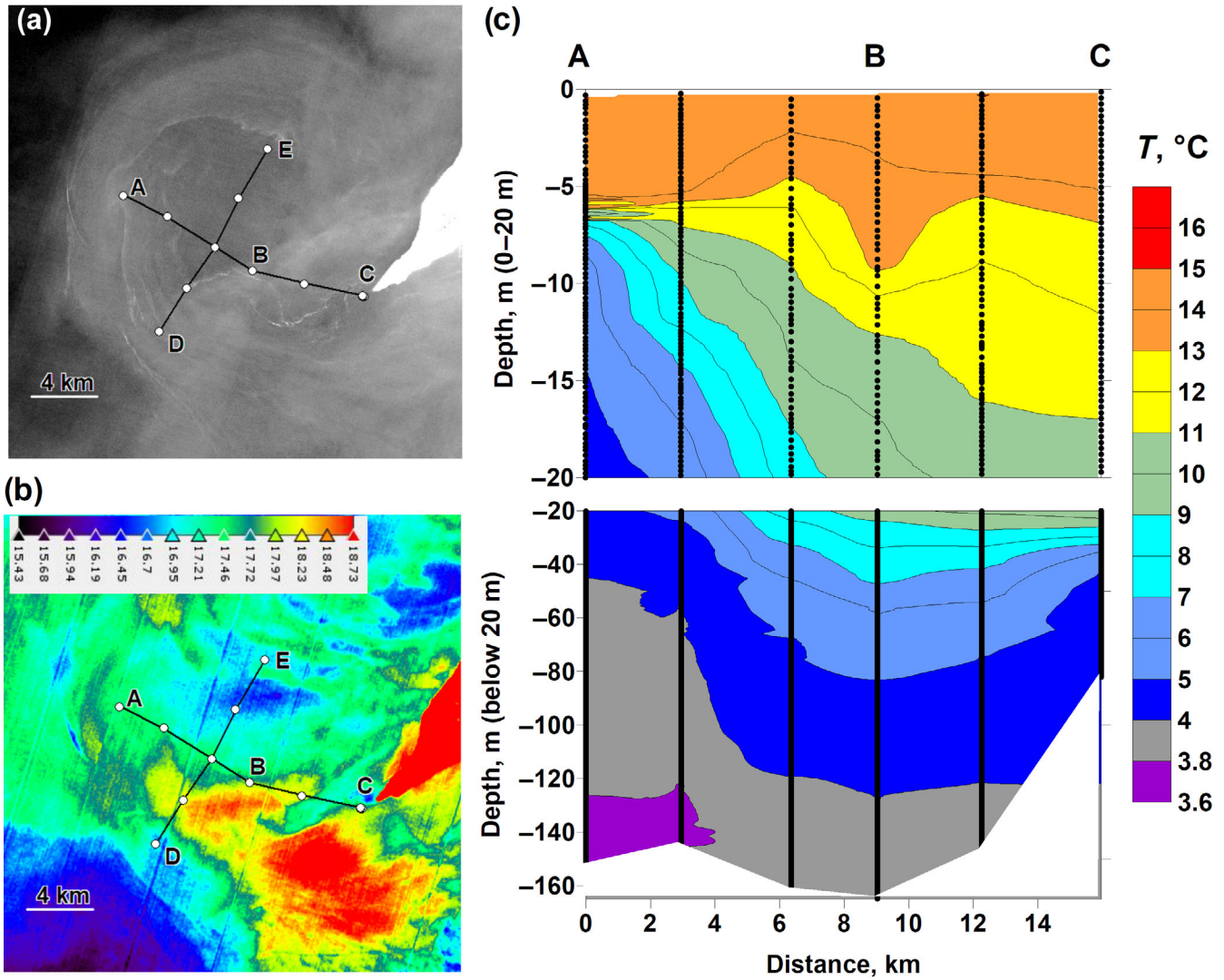


Fig. 4. Landsat 8 images for August 3, 2017 14 h 46 m local time: (a) visible range (band 3, red), and (b) surface temperature (band 10, thermal infrared). (c) Vertical transect of water temperature ($^{\circ}\text{C}$), along the A–C transect (July 31, 2017, between 16 and 20 h local time). Vertical lines indicate station positions. Vertical scale varies for 0–20 m layer and the one below 20 m. Maximal depth is different due to boat drift.

a non-scientific audience: fishermen, tourism agencies, tourists, journalists, and local administration.

Structure and spatial location of eddies

Both the size of the eddies and their temperature difference with the surrounding waters change quite a lot before and after the autumnal overturn. In summer, outflow of warm water from the bay leads to the formation and growth of a warm eddy in July (Fig. 1, region A). Its diameter increases and may reach 35 km by August–September (Fig. 1, region B). Vertical profiles from the boat show that lateral intrusion of water with different temperature and density leads to the deformation of vertical temperature distribution compared with neighboring regions. Accommodation of a new volume of water at the surface will lead to increased thickness (larger vertical

distance between isotherms) of a layer with this temperature and to downward inclination of isotherms below this layer. Repeated influx of warmer, lower density water will lead to downward inclination of isotherms and increased thickness of layers with this specific temperature (see Fig. 4c). Temperature profiles also show that for an anticyclonic eddy formed near the cape in 2017 and for a smaller associated cyclonic eddy in 2019 the water column was affected down to 160 and 80 m, respectively. This illustrates that the eddies observed at the lake surface from satellite imagery are not shallow. They present significant vertical temperature/density gradients, and they have structure and characteristics similar to oceanic eddies.

The duration and the amount of influx to the eddy may also be important factors determining its size. A sustained inflow from the bay (July–October) provides enough volume

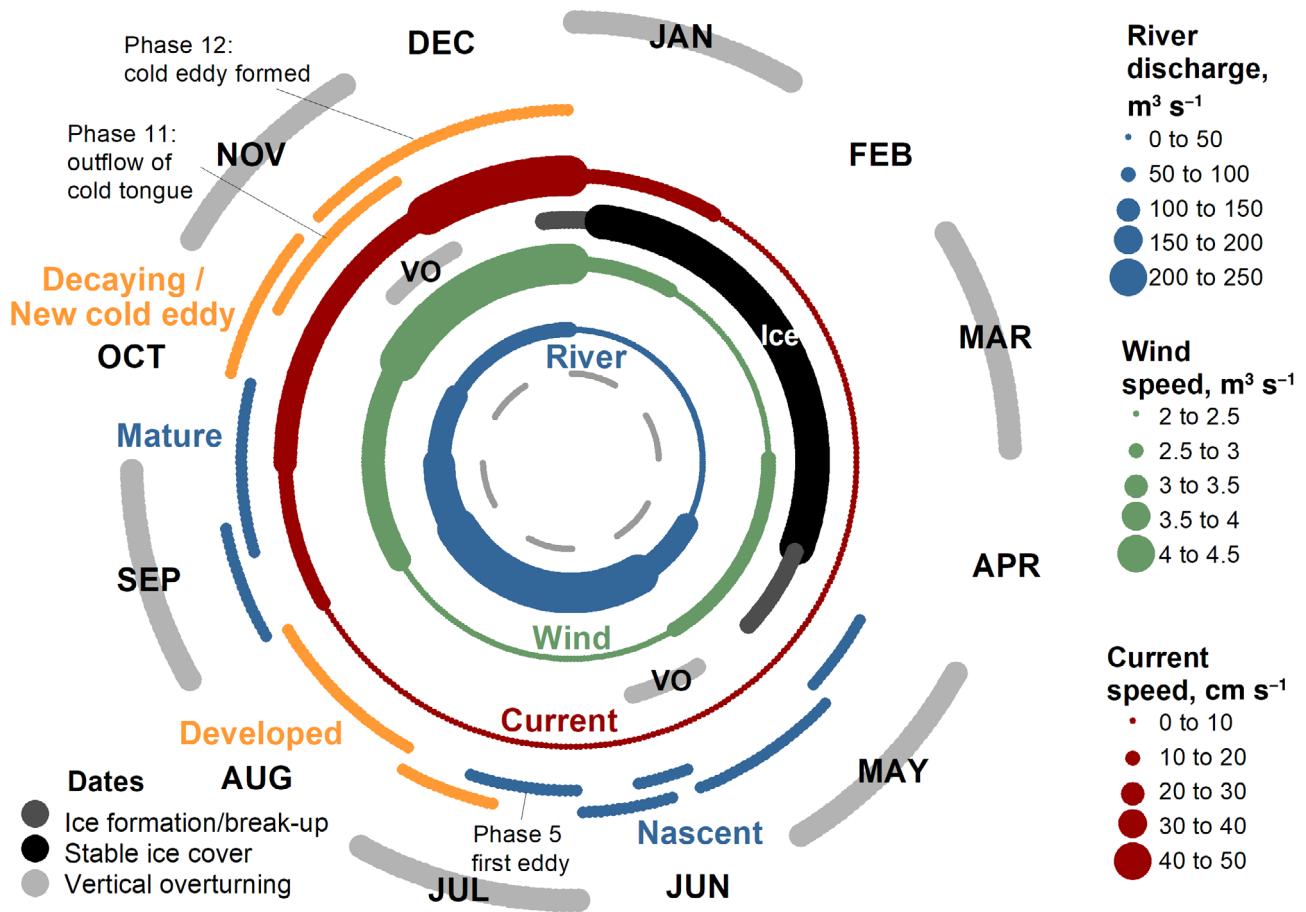


Fig. 5. Radial plot of various natural parameters. Angle represents time, that is, 1 yr = 360°. Inward to outward: monthly mean Barguzin River discharge ($\text{m}^3 \text{s}^{-1}$), average monthly wind speed for five meteorological stations, m s^{-1} ; dates of vertical overturning (marked as “VO”) and ice formation/break-up (2018–2020); median monthly current speed at the mooring station for 2018–2020, cm s^{-1} ; stages (1–12) and four phases (alternating color) of eddies seasonal evolution. Length and position of each stage corresponds to its start and end (see Table 1; Supporting Information Table S2). Odd and even stages are slightly shifted by distance from center to illustrate overlap in time.

for a large warm eddy (35–40 km, see also Fig. 1). An energetic but short inflow (October–December) is consistent with smaller eddies (15–20 km, see Fig. 3m–p). Our data indicate that in the early stage of development both warm and cold mesoscale anticyclonic eddies are located close to the cape. Well-developed warm eddies do not always maintain their position and shape, and are sometimes displaced by 5–15 km (see Fig. 3k–m).

One of implications of our work is better understanding of the generation mechanisms of intrathermocline eddies that are generated in late autumn and persist under ice cover in winter. The location of these eddies after the formation of ice cover can be evaluated either during field surveys, or indirectly from the position of the giant ice rings. If the eddy is quasi-stationary, it may lead to the formation of a giant ice ring. This was documented in 2016 (Kouraev et al. 2016), 2018, and 2019 (Icerings Website, 2024), when the position of the eddy, detected in situ first in mid-February and then in end of March, corresponded to the position of a giant ice ring. A

moving eddy may not necessarily result in ice ring formation, such as we documented in winter 2016/2017 (Kouraev et al. 2019). In some cases advecting eddies may generate ice rings but only in the final stage of ice melt, when the ice is thin. This was the case when ice rings were observed not long before ice break-up in various regions between the cape and Ol’khon Island in 2005, 2013, and 2016 (Kouraev et al. 2019). So for our study region cold eddies are more numerous than the observed ice rings, and it is likely that every year there will be *at least* one cold eddy formed by the end of autumn prior to ice cover formation.

Our results (Kouraev et al. 2016, 2019; Icerings Website, 2024) show that giant ice rings and thus associated intrathermocline eddies are typically tightly clustered in a well-defined zone above the head of underwater depression between the Akademicheskoy Ridge and the Svyatoy Nos Peninsula (see Fig. 1, region C). A similar situation is observed in lakes Hovsgol (Mongolia) and Teletskoye (Russia) where ice rings have been detected over the deepest parts of the lake

(Kouraev et al. 2016, 2019). Anticyclonic vortices are associated with low potential vorticity and due to the dynamical conservation of this quantity tend to lock onto areas having low potential vorticity, such as topographic depressions (see for instance Zhmur, Novoselova, and Belonenko 2022).

This trapping effect of the bathymetry could also be the reason for the large number of ice rings observed in other regions of Lake Baikal, such as Cape Krestovskiy in the southern part of Middle Baikal or Slyudyanka/Kultuk in the western part of Southern Baikal (Kouraev et al. 2016, 2019, 2021). In these two regions, ice rings (and thus intrathermocline eddies) are also located over the heads of underwater depressions.

Conclusions

The generation and horizontal displacement of eddies in dimictic lakes can influence vertical and horizontal exchange of energy, mass, and nutrients, as well as various hydrochemical and biological processes. Similar processes of eddy generation under the influence of river input, wind stress, and coastline shape may well exist in other dimictic lakes but have not yet been observed. Their detection from satellite imagery may be complicated by cloud cover, especially for cold eddies during autumn, or also by unstable or drifting ice cover that does not permit intrathermocline eddies to generate giant ice rings.

Further research using satellite imagery in different parts of the electromagnetic spectrum will potentially provide further insight, especially with recent Surface Water and Ocean Topography radar altimetry mission that provides two-dimensional water topography (SWOT, Fu et al. 2024). Increased temporal frequency of observations and thermal images with better spatial resolution will come from upcoming satellite missions like Thermal Infrared Imaging Satellite for High-resolution Natural Resource Assessment (TRISHNA, launch planned in 2025), Surface Biology and Geology (SBG, launch planned in 2027), Land Surface Temperature Monitoring (LSTM, launch planned in 2029) (Roujean et al. 2021). Satellite data, complemented by numerical modeling and in situ data from boat cruises and loggers, will hopefully provide new information on the three-dimensional structure of the eddies, current field, trajectories, their generation mechanisms, lifecycle, role in horizontal and vertical heat exchange, and impact on the chemistry and biology of the lakes.

Author Contributions

A.V.K., R.E.Z. and A.Ya.S. designed the field work, performed the measurements, and conducted quality control. A.V.K., A.G.K. and A.I.G. analyzed the satellite imagery. A.V.K., E.A.Z., and F.R. analyzed the data. A.V.K., E.A.Z., A.G.K., and N.M.J.H. drafted the first manuscript. All authors contributed to the final version. All authors listed in the manuscript are aware of its submission. The manuscript reports original scientific research; the main results and conclusions have not been published or submitted elsewhere.

Acknowledgments

We would like to thank A. Beketov and I. Kirpichev (Ust-Barguzin, Russia), G. Sibiryakova (Khuzhir, Russia) for help with organizing field work and discussions on wind regime. Heartful thanks to M. Makarov, K. Kucher, R. Gnatovskiy (Irkutsk, Russia), and the team of Limnological Institute, Siberian Branch of the Russian Academy of Sciences (RAS) (Irkutsk) onboard R/V “Vereshagin” for the recovery of the mooring station near the Nizhneye Izgolovye Cape in heavy seas conditions in September 2020. We thank two anonymous reviewers and editorial team of *Limnology and Oceanography* (K. D. Hambright and S. MacIntyre) for the time and attention dedicated to the manuscript and for their constructive remarks. We acknowledge the use of imagery from the National Aeronautics and Space Administration (NASA) Worldview application (<https://worldview.earthdata.nasa.gov>), part of the NASA Earth Observing System Data and Information System (EOSDIS). Sentinel-1 images are from Modified Copernicus Sentinel data (2019–2020)/Sentinel Hub. The Landsat 5, 7, 8, and 9 images are courtesy of the US Geological Survey. Analysis of eddies phases and layout of Fig. 3 were inspired by Grisha Bruskin’s painting “Fundamental Lexicon” (1988). This research was supported by the Centre National d’Etudes Spatiales (CNES) TOSCA LAKEDDIES, TRISHNA, and SWIRL projects. A. G. Kostianoy and A.I. Ginzburg were supported in the framework of the Shirshov Institute of Oceanology Russian Academy of Sciences budgetary financing (Project No. FMWE-2024-0016). E.A. Zakharova was supported in the framework of the Institute of Water Problems, Russian Academy of Sciences budgetary financing (Project No. FMWZ-2022-0001).

References

- Afanasyev, A. N., and V. I. Verbolov, eds. 1977. Currents in Lake Baikal, 159. Novosibirsk, Russia: Nauka.
- Aleskerova, A., A. Kubryakov, S. Stanichny, et al. 2021. “Characteristics of Topographic Submesoscale Eddies Off the Crimea Coast From High-Resolution Satellite Optical Measurements.” *Ocean Dynamics* 71: 655–677. <https://doi.org/10.1007/s10236-021-01458-9>.
- Alpers, W., P. Brandt, A. Lazar, et al. 2013. “A Small-Scale Oceanic Eddy Off the Coast of West Africa Studied by Multi-Sensor Satellite and Surface Drifter Data.” *Remote Sensing of Environment* 129: 132–143. <https://doi.org/10.1016/j.rse.2012.10.032>.
- Bushuev, A. V., N. A. Volkov, and V. S. Loshilov. 1974. Atlas of Ice Formations, 136. Leningrad: Hydrometeoizdat Publishers. (In Russian).
- D’Asaro, E. A., A. Y. Shcherbina, J. M. Klymak, et al. 2018. “Ocean Convergence and the Dispersion of Flotsam.” *Proceedings of the National Academy of Sciences of the United States of America* 115: 201718453. <https://doi.org/10.1073/pnas.1718453115>.

- ESA SNAP Software. 2024. “SNAP download.” <https://step.esa.int/main/download/snap-download/>.
- Fedorov, K. N., and A. I. Ginsburg. 1986. “Mushroom-Like Currents (Vortex Dipoles) in the Ocean and in a Laboratory Tank.” *Annales Geophysicae* 4, no. B5: 507–516.
- Fedorov, K. N., and A. I. Ginsburg. 1992. *The Near-Surface Layer of the Ocean*, 259. Utrecht, The Netherlands and Tokyo, Japan: VSP BV.
- Fu, L.-L., T. Pavelsky, J.-F. Crétaux et al. 2024. “The Surface Water and Ocean Topography Mission: A breakthrough in radar remote sensing of the ocean and land surface water.” *Geophysical Research Letters*, 51, e2023GL107652. <https://doi.org/10.1029/2023GL107652>
- Garmaev, E. Z., and A. V. Khristophorov. 2010. *Water Resources of Rivers From Lake Baikal Watershed: Bases for Their Use and Protection*, 227. Novosibirsk, Russia: Geo Publishing. (In Russian).
- Gibson, W. 2011. *Pattern Recognition*, 356. London, UK: Penguin Books.
- Granin, N. G., V. V. Kozlov, E. A. Tsvetova, and R. Y. Gnatovsky. 2015. “Field Studies and Some Results of Numerical Modeling of a Ring Structure on Baikal Ice.” *Doklady Earth Sciences* 461, no. 1: 316–320. <https://doi.org/10.1134/S1028334X15030204>.
- Grechishev, E. K., and N. V. Mamontov. 1964. “Wave Regime of Lake Baikal.” In *Study of Coasts of Reservoirs and Lake Baikal*, edited by E. K. Grechishev, 17–31. Moscow, Russia: Nauka Publishers. (In Russian).
- Icerings Website. 2024. “The World of the Ice Rings”. Accessed 5 April 2024 www.icerings.org.
- Ivanov, A. Y., and A. I. Ginzburg. 2002. “Oceanic Eddies in Synthetic Aperture Radar Images.” *Journal of Earth System Science* 111, no. 3: 281–295. <https://doi.org/10.1007/BF02701974>.
- Jain, A. K., and R. P. W. Duin. 2004. “Introduction to Pattern Recognition.” In *The Oxford Companion to the Mind*, edited by R. L. Gregory, 2nd ed., 698–703. Oxford, UK: Oxford University Press.
- Kostianoy, A. G., and I. M. Belkin. 1989. “A Survey of Observations on Intrathermocline Eddies in the World Ocean.” In *Mesoscale/Synoptic Coherent Structures in Geophysical Turbulence*, edited by J. C. J. Nihoul and B. M. Jamart, 821–841. Amsterdam, The Netherlands: Proceedings of 20th International Liege Colloquium Ocean Hydrodynamics, Elsevier.
- Kostianoy, A. G., A. I. Ginzburg, O. Y. Lavrova, and M. I. Mityagina. 2018. “Satellite Remote Sensing of Submesoscale Eddies in the Russian Seas.” In *The Ocean in Motion*, edited by M. G. Velarde, R. Tarakanov, and A. Marchenko, 397–413. Cham, Switzerland: Springer Oceanography. Springer. https://doi.org/10.1007/978-3-319-71934-4_24.
- Kostianoy, A. G., and O. Y. Lavrova. 2022. “Satellite Instrumentation and Technique for Oil Pollution Monitoring of the Seas.” In *Instrumentation and Measurement Technologies for Water Cycle Management*, edited by A. Di Mauro, A. Scozzari, and F. Soldovieri, 53–77. Cham, Switzerland: Springer Nature. https://doi.org/10.1007/978-3-031-08262-7_4.
- Kouraev, A. V., E. A. Zakharova, A. G. Kostianoy, et al. 2021. “Giant Ice Rings in Southern Baikal: Multi-Satellite Data Help to Study Ice Cover Evolution and Eddies Under Ice.” *The Cryosphere* 15: 4501–4516. <https://doi.org/10.5194/tc-15-4501-2021>.
- Kouraev, A. V., E. A. Zakharova, F. Rémy, et al. 2016. “Giant Ice Rings on Lakes Baikal and Hovsgol: Inventory, Associated Water Structure and Potential Formation Mechanism.” *Limnology and Oceanography* 61: 1001–1014. <https://doi.org/10.1002/lno.10268>.
- Kouraev, A. V., E. A. Zakharova, F. Rémy, et al. 2019. “Giant Ice Rings on Lakes and Field Observations of Lens-Like Eddies in the Middle Baikal (2016–2017).” *Limnology and Oceanography* 64: 2738–2754. <https://doi.org/10.1002/lno.11338>.
- Landsat Product Website. 2024. “Landsat products”. Accessed 5 April 2024 <https://landsat.usgs.gov/>.
- Lavrova, O., A. G. Yu, S. A. Kostianoy, M. I. Lebedev, A. I. G. Mityagina, and N. A. Sheremet. 2011. *Complex Satellite Monitoring of the Russian Seas*, 470. Moscow, Russia: IKI RAN. (in Russian).
- Le Core, H. L. 1998. “Use of Numerical Models and Satellite Data to Study Physical Processes in Lake Baikal.” Thesis Submitted for the Degree of Doctor of Philosophy at the University of Leicester, Leicester, 136.
- Leech, D. M. 2018. “Satellites and Sensors Tell Us More About the Giant Ice Rings of Siberian Lakes.” *Limnology and Oceanography Bulletin* 27, no. 4: 119–120. <https://doi.org/10.1002/lob.10278>.
- Maio, C. V., J. P. Donnelly, R. Sullivan, et al. 2016. “Sediment Dynamics and Hydrographic Conditions During Storm Passage, Waquoit Bay, Massachusetts.” *Marine Geology* 381: 67–86. <https://doi.org/10.1016/j.margeo.2016.07.004>.
- Pattiaratchi, C., A. James, and M. Collins. 1986. “Island Wakes and Headland Eddies: A Comparison Between Remotely Sensed Data and Laboratory Experiments.” *Journal of Geophysical Research* 92, no. C1: 783–794. <https://doi.org/10.1029/JC092iC01p00783>.
- Robinson, A. R., ed. 1983. *Eddies in Marine Science*, 609. Berlin, Heidelberg: Springer.
- Roujean, J.-L., B. Bhattacharya, P. Gamet, et al. 2021. “TRISHNA: An Indo-French Space Mission to Study the Thermography of the Earth at Fine Spatio-Temporal Resolution.” In *IEEE International India Geoscience and Remote Sensing Symposium (InGARSS)*, vol. 2021, 49–52. Ahmedabad, India: IEEE. <https://doi.org/10.1109/InGARSS51564.2021.9791925>.
- Rusineck, O. T., V. V. Takhteev, D. P. Gladkochub, et al. 2012. *Baicalogy: In 2 Books*, 468. Novosibirsk, Russia: Nauka Publishers. (In Russian).
- Rzheplinskiy, G. V., and A. I. Sorkina, eds. 1977. *Wind and Wave Atlas of Lake Baikal*, 117. Leningrad, Russia: Hydrometeoizdat Publishing. (In Russian).

- Sheremet, V. A. 2010. "SeaHorse Tilt Current Meter: Inexpensive Near Bottom Current Measurements Based on Drag Principle with Coastal Applications." *Eos*, Portland, Oregon USA, Transactions of the American Geophysical Union, 91 (26) (Ocean Sci. Suppl.): PO25C-13 (Abstract).
- Shimaraev, M. N., and V. I. Verbolov. 1998. "Water Temperature and Circulation." In *Lake Baikal: Evolution and Diversity*, edited by O. M. Kozhova and L. R. Izmet'seva, 26–44. Leiden: Backhuys Publishers.
- Smirnov, V. G., ed. 2011. *Satellite Methods for Studies of Sea Ice Cover*, 239. St Petersburg, Russia: AARI. (In Russian).
- Stopa, E., A. A. Mouche, B. Chapron, and F. Collard. 2017. "Sea State Impacts on Wind Speed Retrievals From C-Band Radars." *IEEE Journal of Selected Topics in Applied Earth Observations and Remote Sensing* 10, no. 5: 2147–2155. <https://doi.org/10.1109/JSTARS.2016.2609101>.
- Sutyryna, E. N. 2016. "The Study of Vortex Structures in Lake Baikal Using Remote Sensing Data." *International Research Journal* 4: 157–159. (In Russian). <https://doi.org/10.18454/IRJ.2016.49.109>.
- Troitskaya, E., V. Blinov, V. Ivanov, et al. 2015. "Cyclonic Circulation and Upwelling in Lake Baikal." *Aquatic Sciences* 77, no. 2: 171–182. <https://doi.org/10.1007/s00027-014-0361-8>.
- Villas Bôas, A. B., F. Ardhuin, A. Ayet, et al. 2019. "Integrated Observations of Global Surface Winds, Currents, and Waves: Requirements and Challenges for the Next Decade." *Frontiers in Marine Science* 6: 425. <https://doi.org/10.3389/fmars.2019.00425>.
- Zatsepin, A. G., A. Kubryakov, A. Aleskerova, D. Elkin, and O. Kukleva. 2019. "Physical Mechanisms of Submesoscale Eddies Generation: Evidences From Laboratory Modeling and Satellite Data in the Black Sea." *Ocean Dynamics* 69: 253–266. <https://doi.org/10.1007/s10236-018-1239-4>.
- Zhmur, V. V., E. V. Novoselova, and T. V. Belonenko. 2022. "Peculiarities of Formation of the Density Field in Mesoscale Eddies of the Lofoten Basin: Part 2." *Oceanology* 62: 289–302. <https://doi.org/10.1134/S0001437022030171>.

Supporting Information

Additional Supporting Information may be found in the online version of this article.

Submitted 17 June 2024

Revised 31 August 2024

Accepted 21 December 2024